Synthesis, properties and X-ray crystal structure of a new heteropolyacid supermolecular charge-transfer complex [(VB$_1$)$_2$DMFHPMo$_{12}$O$_{40}$·5DMF]

Shizhong Liu,[a]* Jianping Li,[a] Xianhua Feng,[a] Zhengtai Cao,[a] Zhenwen Zhang,[a] Zheng Wang,[a] Yan Xing,[b] Hengqing Jia[b] and Yonghua Lin[b]

[a]Faculty of Chemistry and Material Science, Hubei University, Wuhan 430062, People's Republic of China, and [b]Changchun Institute of Applied Chemistry, Chinese Academy of Science, Changchun 130022, People's Republic of China

Correspondence e-mail: liuq11@public.wh.hb.cn

The title complex [(VB$_1$)$_2$DMFHPMo$_{12}$O$_{40}$·5DMF, VB$_1$ = vitamin B$_1$ (thiamine chloride), DMF = *N*,*N*-dimethylformamide] has been synthesized and characterized by elemental analysis, IR, UV-Vis, electron spin resonance, X-ray photoelectron spectroscopy and cyclic voltammetry methods. The X-ray crystal structure revealed that there is one independent molecule in the unit cell of the title complex that contains one mixed-valence heteropolyanion, two VB$_1^+$ cations and six DMF molecules. The title complex possesses a centrosymmetrical arrangement in the unit cell, with the P atom at the symmetry center of the heteropolyanion and with eight O atoms surrounding the central P atom, such that two sets of PO$_4$ tetrahedra are formed. The PO$_4$ tetrahedra and MoO$_6^{6-(7-)}$ octahedra are disordered in the heteropolyanion. The bond distances of P—O$_a$ and Mo≡O$_d$ are in the ranges 1.57 (4)–1.70 (4) Å and 1.61 (2)–1.67 (2) Å, respectively.

1. Introduction

In recent years, the design, synthesis and application of functional molecular materials has posed a major scientific challenge. One type of these materials, organic polyoxometalate hybrid materials, are increasingly receiving attention from materials scientists and chemists because of their optical, electrical, magnetic and thermal properties.

Ouahab *et al.* (1988) first used a π-electron donor molecule, tetrathiafulvalene (TTF), as an organic donor to combine with polyoxometalate [PW$_{12}$O$_{40}$]$^{3-}$ and successfully synthesized a novel organic–polyoxometalate charge-transfer complex, (TTF)$_6$PW$_{12}$O$_{40}$(Et$_4$N)$_2$. They studied its structure, features, conductivity and magnetic properties. Later, they prepared bis(ethylenedithio)tetrathiafulvalene (ET) hexamolybdate and ET hexatungstate salts (ET)$_2$$M_6O_{19}$, M = Mo, W. These complexes not only possess interesting optical, electrical and magnetic characteristics but also possess potential antiviral activity (Ouahab *et al.*, 1988; Triki *et al.*, 1991; Pope & Müller, 1994; Coronado & Gomez-Garcia, 1998; Sanchez *et al.*, 1982).

Polyoxometalates that are used as inorganic components in organic–inorganic hybrid materials have the following characteristics:

(i) Heteropolyacid anions have well defined shapes and sizes and high charges. They can induce organic components to be self-assembled by different means. This kind of interaction between organic components and heteropolyanions is important in polyoxometalate molecular biology.

(ii) Polyoxometalates have multi-stage redox states. As strong electron acceptors, their redox potentials make them suitable for reaction with the organic donor TTF. They are soluble in water and are organic solvents. Furthermore, they can form assemblies with organic components.

(iii) Polyoxometalates are strong oxidants. They can receive electrons to be reduced to mixed-valence states without changing their shape, the electron delocalization of the organic systems or the spin localization in the inorganic systems.

(iv) The geometrical configuration, electronic versatility and pattern of assembly with the organic components can be modified by changing the composition of polyoxometalates.

(v) The reduction products of polyoxometalates, namely heteropoly blues, have good thermal stability and good stability in aqueous solution.

The electron donors of most hybrid molecular materials are organic molecules of the TTF or ET type (So & Pope, 1992), organometallic decamethylferrocene (Zhang *et al.*, 1997), organic amine (Wang *et al.*, 1992) *etc.* However, the use of heterocyclic compounds containing S and N atoms has not been reported. Vitamin B_1 is an *S,N*-heterocycle that has important functions in sugar metabolism. In order to obtain organic–polyoxometalate hybrid medicines with antiviral activity, we synthesized a charge-transfer complex by chemical self-assembly, using the heteropolyacid $H_3PMo_{12}O_{40}$ as the host and vitamin B_1 as the guest. We also report its characterization by spectroscopic and single-crystal diffraction methods.
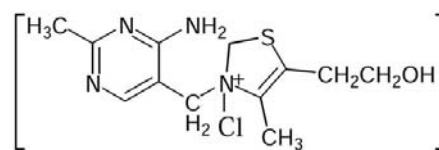
2. Experimental

2.1. Materials

All chemicals were analytical grade and were used without further purification. Distilled water was used throughout the work.

2.2. Measurements

Elemental analyses were performed on a Carlo Erba 1106 analytical instrument. Infrared spectra were recorded as KBr discs on a Nicolet FT-IR-410 instrument. Electronic spectra were obtained on a Shimadzu UV-250IPC spectrometer at 77 K, and X-ray photoelectron spectroscopy was performed on a KRATOS XSAM800. Cyclic voltammetry was performed using a BAS-100A electrochemical analysis system, with a Pt trap as working electrode, a coiled Pt wire as counter electrode and an Ag/AgCl reference electrode.

2.3. Synthesis of (VB$_1$)$_2$DMFHPMo$_{12}$O$_{40}$·5DMF

$H_3PMo_{12}O_{40}$ (0.1 mmol, 1.83 g) and VB_1 (0.3 mmol, 1.01 g) were mixed in water (30 cm^3) and then stirred for 2 h until a dark-green precipitate appeared. After filtering by suction and washing with distilled water three times, the deep-green crystals of the title complex were isolated by recrystallization from DMF/H$_2$O (v/v = 3/1) several days later. Elemental analysis results were as follows: C 17.82%, H 2.57%, N 6.69%; calculated for $C_{42}H_{76}Mo_{12}N_{14}O_{52}PS_2$: C 17.66%, H 2.68%, N 6.87%. The VB_1 cation is shown below.

2.4. Crystal structure determination

A deep-green prism crystal of size $0.5 \times 0.42 \times 0.40$ mm was used for data collection. The data were collected at room temperature using a Siemens P4 four-circle diffractometer with graphite monochromated Mo $K\alpha$ radiation ($\lambda = 0.71073$ Å), using ω–2θ scan mode in the range $1.54 \le \theta \le 23.02°$. Of a total of 6706 unique reflections, 5563 had $I > 2\sigma(I)$. All data were corrected for L_p (Lorentz and polarization) factors and empirically for absorption.

The crystal structure was solved by the *SHELXTC-PC* procedure on a 486 personal computer. The heavy-atom coordinates were located by direct methods. While non-H atoms were refined by full-matrix least-squares methods using *SHELXTL*, the H-atom positions were assigned using geometrical considerations. The crystallographic data are summarized in Table 1.

3. Results and discussion

3.1. Infrared spectrum

The IR data and assignment for the title compound and $H_3PMo_{12}O_{40}$ are listed in Table 2. It can be seen that the related vibration bands of the heteropolyanion remain almost unchanged in the structure of the title complex. Comparing the IR spectra of the title compound with those of $H_3PMo_{12}O_{40}$, we observed that the vibration band of P—O$_a$ in the title compound had undergone a blue shift, from 1067 (vs) cm^{-1} to 1079 (vs) cm^{-1}. The bonds of M=O$_d$ and Mo—O$_b$—Mo both have blue shifts from 975 (s) cm^{-1} and 870 (w) cm^{-1} to 979.6 (s) cm^{-1} and 895 (w) cm^{-1}, respectively. The vibration band of Mo—O$_c$—Mo had undergone a red shift, from 810 (vs) cm^{-1} to 800.3 (vs) cm^{-1}. The results indicate the presence of a partial charge-transfer interaction between the VB_1 organic donor and the heteropolyanion acceptor. The bonds D—O$_a$, Mo=O$_d$ and Mo—O$_b$—Mo were strengthened and the Mo—O$_c$—Mo bonds were weakened after the anion was reduced in the title compound. The four Mo$_3$O$_{13}$ groups surround the central P heteroatom tetrahedrally, in such a way that the full unit has T_d symmetry. This situation is rare in salts containing $XMo_{12}O_{40}{}^{n-}$, which easily form disordered pseudo-Keggin polyoxoanions (Evans & Pope, 1984).

3.2. Ultraviolet spectra

The diffuse reflectance electronic spectrum of the title compound is presented in Fig. 1. The absorption band at 789 nm is assigned to the intervalence charge-transfer transition Mo(V) $\rightarrow$ Mo(VI) of the reduced anion $PMo_{12}O_{40}{}^{4-}$,

Table 1
Experimental details.

Crystal data	
Chemical formula	$C_{42}H_{76}Mo_{12}N_{14}O_{52}PS_2$
Chemical formula weight	2855.54
Cell setting, space group	Triclinic, $P\bar{1}$
a, b, c (Å)	12.322 (3), 13.607 (3), 14.160 (3)
α, β, γ (°)	103.900 (3), 98.87 (3), 112.85 (3)
V (Å^3)	2040.9 (7)
Z	1
D_x (Mg m^{-3})	2.323
Radiation type	Mo $K\alpha$
No. of reflections for cell parameters	23
θ range (°)	4.89–9.73
μ (mm^{-1})	1.958
Crystal color	Deep green
Crystal size (mm)	$0.50 \times 0.42 \times 0.40$
$F(000)$	1156
Data collection	
T_{min}	0.50034
T_{max}	0.99156
No. of measured, independent and observed parameters	6706, 5563, 4509
Criterion for observed reflections	$I > 2\sigma(I)$
R_{int}	0.0792
θ_{max} (°)	23.02
Range of h, k, l	$-1 \rightarrow h \rightarrow 13$
	$-13 \rightarrow k \rightarrow 13$
	$-15 \rightarrow l \rightarrow 15$
Refinement	
Refinement on	F^2
$R[F^2 > 2\sigma(F^2)]$, $wR(F^2)$, S	0.0893, 0.2188, 1.198
No. of reflections and parameters used in refinement	5407, 552
Weighting scheme	$w = 1/[\sigma^2(F_o^2) + (0.1012P)^2 + 51.6101P]$ where $P = (F_o^2 + 2F_c^2)/3$
$(\Delta/\sigma)_{max}$	3.172
$\Delta\rho_{max}, \Delta\rho_{min}$ (e Å^{-3})	1.349, -1.631
Extinction method	SHELXL
Extinction coefficient	0.0159 (11)

Computer programs used: *SHELXS*86 (Sheldrick, 1990), *SHELXL*93 (Sheldrick, 1993).

which indicates that electrons transfer between vitamin B_1 and $[PMo_{12}O_{40}]^{3-}$, converting $[PMo_{12}O_{40}]^{3-}$ to the heteropoly blue $[PMo_{12}O_{40}]^{4-}$. This is direct evidence of the formation of a charge-transfer complex. The absorption bands at 431 nm and 376 nm are ascribed to $O_{b(c)} \rightarrow Mo$ and $O_d \rightarrow Mo$ transitions, respectively.
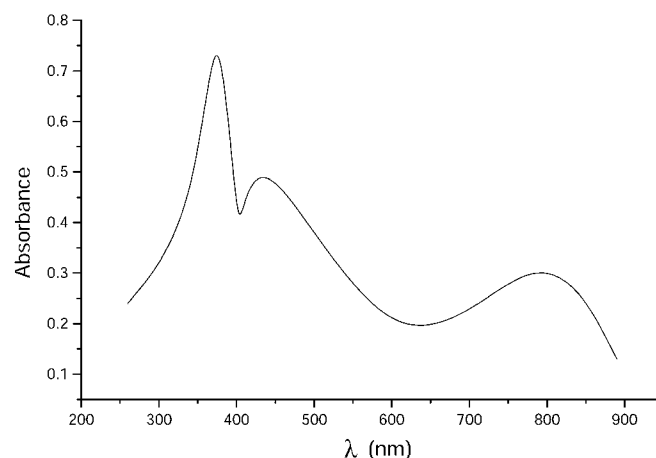
3.3. Electron spin resonance spectra

The ESR spectrum of the title compound irradiated by UV light for 1 h at 77 K is shown in Fig. 2. The spectrum reveals the presence of a single isotropic paramagnetic signal $g = 1.935$, which is ascribed to Mo^{5+}. This shows that the heteropolyanions have each undergone a one-electron reduction. The presence of an unpaired electron trapped on a single Mo atom ($Mo\!=\!O_d \simeq 1.7$ Å) with $g_\perp > g_\parallel$ ($g_\perp = 1.974$, $g_\parallel = 1.918$) suggests that the MoO_6 octahedra in the heteropolyanions are distorted, the distortion axis (a) lying along the shortest $Mo\!=\!O_d$ double bond. The hyperfine lines are not observed since the temperature at which the spectrum was
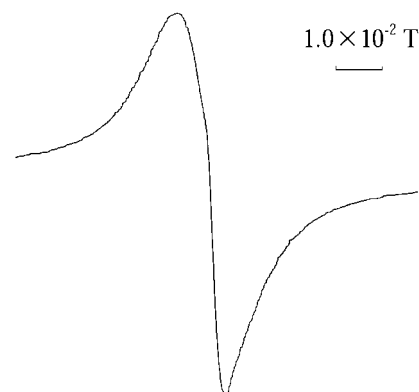
recorded (77 K) was not low enough. The hyperfine structure disappeared and the central line of the ESR spectra broadened as the temperature was raised from 45 K to 120 K. This indicates that the electron is hopping among Mo atoms and that the high mobility of the unpaired electron is comparable to the ESR time scale (Sanchez *et al.*, 1982; So & Pope, 1992).

3.4. X-ray photoelectron spectroscopy study

The XPS data of related compounds for S_{2p}, N_{1s}, P_{2p}, Mo_{3d} and O_{1s} are shown in Table 3. The deep-green title compound turned gray-blue when irradiated by a 450 W Hg lamp. The binding energies of Mo_{3d}, P_{2p} and O_{1s} in the title compound are 232.26, 134.64 and 531.67 eV, respectively, which are smaller than those in $H_3PMo_{12}O_{40}$. The results indicate that the binding energy of the title compound decreased, since all Mo atoms are equivalent in both compounds. In terms of class IIA of the Robin & Day (1967) scheme, the existence of reduced molybdenum in the polyoxoanion cannot be ruled out. In that case, the shift in energy should be very small, since the extra electron is delocalized over all the Mo atoms.

Figure 1
Diffusion reflectance electronic spectrum of the title compound.

Figure 2
X-band ESR spectrum of the title complex at 77 K following irradiation for 1 h by a 450 W Hg lamp.

Table 2
IR spectral data for the title complex and the related acid (cm^{-1}).

Compounds	$\nu_{as}P-O_a$	$\nu_{as}Mo=O_d$	$\nu_{as}Mo-O_b-Mo$	$\nu_{as}Mo-O_c-Mo$
$H_3PMo_{12}O_{40}$	1067	975	870	810
[(VB$_1$)$_2$DMF-HPMo$_{12}$O$_{40}$·5DMF]	1079.6	979.6	895	800.3

Table 3
XPS data for the title compound and $H_3PMo_{12}O_{40}$ (eV).

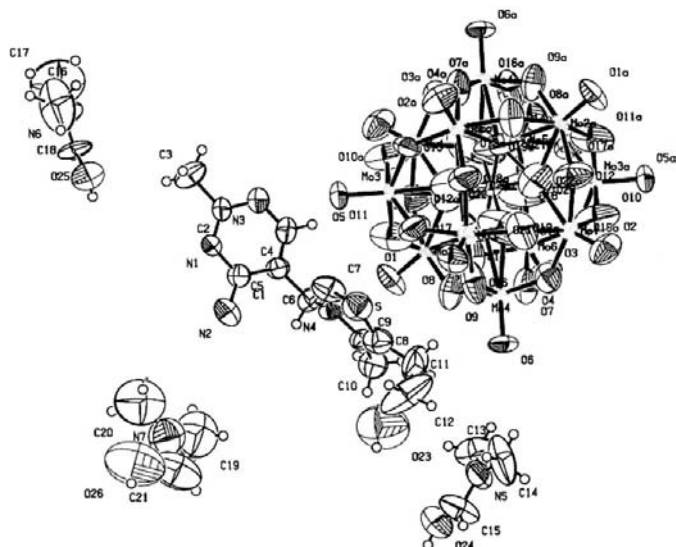|	S_{2p}	N_{1s}	P_{2p}	Mo_{3d}	O_{1s}
[(VB$_1$)$_2$DMF-HPMo$_{12}$O$_{40}$·5DMF]	166.17	400.14	134.64	232.26	531.67
$H_3PMo_{12}O_{40}$			134.8	233.49	531.86

Table 4
CV data of the title complex (mV).

Epc: peak potential of cathodic. *Epa*: peak potential of anodic. ΔEp: separation of cathodic and anodic peaks. *n*: number of electrons. For a reversible *n*-electron reduction, $\Delta Ep = 59$–$63 n^{-1}$ mV.

Epc	Epa	ΔEp	n
−693	−804	−887	1
−585	685	−810	1
108	119	77	1

3.5. Cyclic voltammetry

The redox property of the title complex was tested in the mixed solvents of water and 1,4-dioxane (*v*/*v* = 1/1), using 0.5 mol l^{-1} HCl as the supporting electrolyte. The results (see Table 4) show that the title complex has three pairs of redox peaks with potential differences (ΔEp) of 108, 119 and 77 mV, respectively, corresponding to a reversible process in each of the three one-electron redox steps.
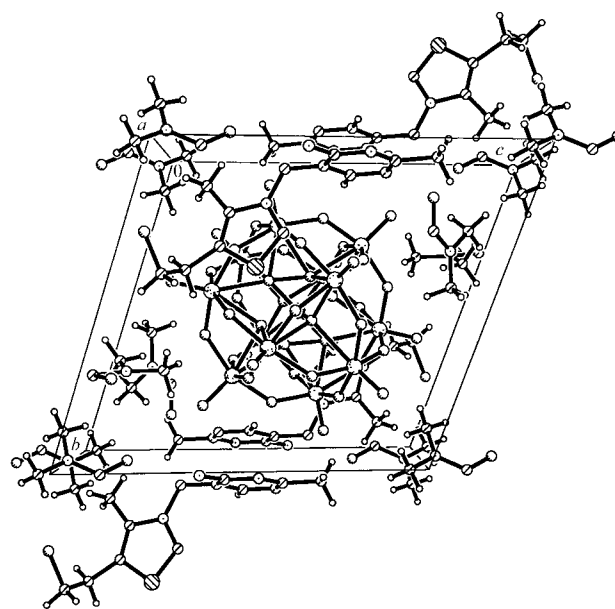

Figure 3
Molecular structure of the title compound.

3.6. X-ray crystal structure

The molecular structure of the title compound and its crystal structure are shown in Figs. 3 and 4, respectively. The coordinates and parameters of some non-H atoms are given in the supplementary material,[1] and bond lengths and bond angles are listed in Tables 5 and 6, respectively.

The title compound consists of two vitamin B$_1$ cations, one PMo$_{12}$O$_{40}$$^{4-}$ heteropolyanion and six DMF molecules. The P atom is at the crystallographic inversion center of the heteropolyanion and eight O atoms surround it (Brown *et al.*, 1977). Each O atom has two equal sites, *i.e.* O(19) and O(19A), O(20) and O(20A), O(21) and O(21A), O(22) and O(22A). The occupancy of each O atom is 0.5 and the coordination number of the P atom is four. The bond lengths of the PO$_4$ unit range from 1.57 (4) Å to 1.71 (4) Å. The bond angles of O—P—O range from 104 (2)° to 115 (2)°. These data suggest that the PO$_4$ tetrahedra are distorted and the P—O bonds are weakened.

In the 12 MoO$_6$ octahedra, the shortest Mo=O$_d$ double-bond lengths range from 1.61 (2) Å to 1.67 (2) Å. The longest Mo—O$_a$ bond lengths range from 2.31 (3) Å to 2.51 (3) Å. The bond lengths of Mo—O$_{b(c)}$ range from 1.84 (2) Å to 1.99 (2) Å. The variation of the bond angles of O$_{b(c)}$—Mo—O$_{b(c)}$ and O$_a$—Mo—O$_d$ ranges from 153.8 (12)° to 162.0 (12)° and from 60.2 (10)° to 104.3 (12)°, respectively. These data indicate that there are significant distortions in the MoO$_6$ octahedra.

Figure 4
Molecular packing of the title compound in the unit cell.

Table 5
Selected bond lengths (Å).

Mo1—O2	1.61 (2)	Mo1—O12	1.86 (2)
Mo1—O10	1.86 (2)	Mo1—O13	1.93 (2)
Mo1—O4	1.95 (2)	Mo1—O19	2.39 (5)
Mo1—O22†	2.46 (4)	Mo2—O1	1.62 (2)
Mo2—O11	1.87 (2)	Mo2—O14	1.95 (2)
Mo2—O12†	1.96 (2)	Mo2—O9	1.96 (2)
Mo2—O21	2.33 (5)	Mo2—O22	2.34 (4)
Mo3—O5	1.67 (2)	Mo3—O10†	1.90 (2)
Mo3—O11	1.93 (2)	Mo3—O15	1.93 (2)
Mo3—O17	1.99 (2)	Mo3—O20†	2.32 (5)
Mo3—O22	2.51 (4)	Mo4—O6†	1.65 (2)
Mo4—O4	1.84 (2)	Mo4—O16	1.87 (2)
Mo4—O9	1.87 (2)	Mo4—O7	1.91 (2)
Mo4—O19	2.31 (3)	Mo4—O21	2.44 (3)
Mo5—O8	1.66 (2)	Mo5—O13	1.85 (2)
Mo5—O17	1.85 (2)	Mo5—O16	1.95 (2)
Mo5—O18†	1.96 (3)	Mo5—O19	2.42 (3)
Mo5—O20†	2.48 (3)	Mo6—O3	1.66 (2)
Mo6—O14	1.85 (2)	Mo6—O15†	1.86 (2)
Mo6—O7	1.88 (2)	Mo6—O18	1.93 (2)
Mo6—O20	2.40 (3)	Mo6—O21	2.49 (3)
P—O22†	1.57 (4)	P—O22	1.57 (4)
P—O21	1.61 (3)	P—O21†	1.61 (3)
P—O20†	1.64 (4)	P—O20	1.64 (4)
P—O19	1.70 (4)	P—O19†	1.70 (4)
O10—Mo3†	1.90 (2)	O12—Mo2†	1.96 (2)
O15—Mo6†	1.86 (2)	O18—Mo5†	1.96 (3)
O20—Mo3†	2.32 (5)	O20—Mo5†	2.48 (3)
O22—Mo1†	2.46 (4)		

† Symmetry transformations used to generate equivalent atoms: $-x + 1$, $-y + 3$, $-z + 1$.

Table 6
Bond angles (°).

O6—Mo4—O16	98.4 (13)	O6—Mo4—O4	101.0 (11)
O6—Mo4—O9	99.2 (11)	O4—Mo4—O16	88.3 (9)
O16—Mo4—O9	88.7 (9)	O4—Mo4—O9	159.8 (10)
O4—Mo4—O7	88.7 (9)	O6—Mo4—O7	102.5 (11)
O9—Mo4—O7	87.0 (8)	O16—Mo4—O7	159.1 (12)
O4—Mo4—O19	63.1 (14)	O6—Mo4—O19	156 (2)
O9—Mo4—O19	98 (2)	O16—Mo4—O19	64.6 (12)
O6—Mo4—O21	158.2 (14)	O7—Mo4—O19	95.7 (11)
O16—Mo4—O21	94.8 (12)	O4—Mo4—O21	96.7 (13)
O7—Mo4—O21	65.0 (9)	O9—Mo4—O21	63.7 (13)
O8—Mo5—O13	103.2 (10)	O19—Mo4—O21	46.0 (14)
O13—Mo5—O17	160.1 (12)	O8—Mo5—O17	96.6 (13)
O13—Mo5—O16	88.9 (9)	O8—Mo5—O16	98.5 (10)
O8—Mo5—O18†	99.5 (12)	O17—Mo5—O16	89.7 (10)
O17—Mo5—O18†	88.7 (10)	O13—Mo5—O18†	86.5 (10)
O8—Mo5—O19	154.2 (13)	O16—Mo5—O18†	162.0 (12)
O17—Mo5—O19	99 (2)	O13—Mo5—O19	63.0 (13)
O18†—Mo5—O19	101.2 (13)	O16—Mo5—O19	61.4 (11)
O13—Mo5—O20†	96.5 (13)	O8—Mo5—O20†	155.3 (12)
O16—Mo5—O20†	96.7 (10)	O17—Mo5—O20†	64.0 (14)
O19—Mo5—O20†	50.0 (14)	O18†—Mo5—O20†	66.6 (11)
O3—Mo6—O15†	99.5 (11)	O3—Mo6—O14	100.4 (11)
O3—Mo6—O7	99.2 (10)	O14—Mo6—O15†	159.9 (10)
O15†—Mo6—O7	90.2 (9)	O14—Mo6—O7	84.2 (9)
O14—Mo6—O18	89.4 (10)	O3—Mo6—O18	99.6 (12)
O7—Mo6—O18	160.9 (12)	O15†—Mo6—O18	89.8 (10)
O14—Mo6—O20	98.4 (13)	O3—Mo6—O20	157.6 (13)
O7—Mo6—O20	94.6 (10)	O15†—Mo6—O20	62.8 (13)
O3—Mo6—O21	155.8 (11)	O18—Mo6—O20	68.6 (11)
O15†—Mo6—O21	98.0 (14)	O14—Mo6—O21	62.3 (12)
O18—Mo6—O21	97.0 (11)	O7—Mo6—O21	64.1 (10)
		O20—Mo6—O21	46.4 (12)

† Symmetry transformations used to generate equivalent atoms: $-x + 1$, $-y + 3$, $-z + 1$.

Generally, the average bond length of Mo—O in the MoO$_6$ octahedra is longest for Mo(V). Thus, the reduced Mo(V) atom in the title complex is Mo(3) or Mo(3A). The bond lengths of the crystals were calculated using the relationship between the bond length (r) and bond valence (S), $S_{ij} = \exp[(r_0 - r_{ij})/B]$, $V_i = \sum S_{ij}$ (Brown & Altermatt, 1985; Schroder, 1975). The calculated data were in good agreement with the experimental results. From the crystal data of the reduced compound, we find that the Mo=O$_d$ bond is stretched, while the four Mo=O$_{b(c)}$ bonds located on the equator are shortened, indicating the formation of a stretched octahedron. Such distortion is caused by the Jahn–Teller effect. It is observed that the Keggin structure of heteropolyanions does not change during the process of reduction.

However, we were unable to find hydrogen bonds in the title compound. Therefore, it is difficult to deduce the mechanism of the charge transfer, although it may have some relationship with the properties of the host–guest (donor–acceptor) compound.

References

Brown, G. M., Noe-Spirlet, M.-R., Busing, W. R. & Levy, H. A. (1977). *Acta Cryst.* B**33**, 1038–1046.

Brown, I. D. & Altermatt, D. (1985). *Acta Cryst.* B**41**, 244–247.

Coronado, E. & Gomez-Garcia, C. J. (1998). *Chem. Rev.* **88**, 273–296.

Evans, H. T. Jr & Pope, M. T. (1984). *Inorg. Chem.* **23**, 501–504.

Ouahab, L., Bencharif, M. & Grandjean, D. (1988). *C. R. Acad. Sci. Paris*, Ser. II, **307**, 749–752.

Pope, M. T. & Müller, A. (1994). *Polyoxometalates from Platonic Solid to Anti-Retroviral Activity*, pp. 1–408. London: Kluwer Academic.

Robin, M. B. & Day, P. (1967). *Adv. Inorg. Chem. Radiochem.* **10**, 247–422.

Sanchez, C., Livage, J. & Launay, J. P. (1982). *J. Am. Chem. Soc.* **104**, 3194–3202.

Schröder, F. A. (1975). *Acta Cryst.* B**31**, 2294–2309.

So, H. & Pope, M. T. (1992). *Electron and Proton Transfer in Chemistry and Biology*, pp. 71–93. Amsterdam: Elsevier Science.

Triki, S., Ouahab, L. & Grandjean, D. (1991). *Acta Cryst.* C**47**, 645–648.

Wang, E. B., Zhang, L. C. & Shen, E. H. (1992). *Sci. China Ser. B*, **7**, 673–682.

Zhang, X. M., Shan, B. Z. & You, X. Z. (1997). *Polyhedron*, **16**, 713–719.